# A Finite Element Method for Transient Analysis of Power Electronic Motor Drives Including Parasitic Capacitive Effect and External Circuit

W. N. Fu and S. L. Ho
The Hong Kong Polytechnic University
Hung Hom, Kowloon, Hong Kong
eewnfu@polyu.edu.hk

***Abstract*—A two dimensional (2-D) finite element method (FEM) of transient electromagnetic field for modeling power electronic motor drives is presented. The proposed method takes into account the parasitic capacitive effect and can be coupled with arbitrarily connected circuits. The FEM formulation which includes the displacement current in the direction of the model's depth is deduced. The displacement current effect in the plane of the solution domain is represented by coupling the circuit of capacitances into the FEM equations. By introducing additional unknowns, the final set of the system equations has a symmetrical coefficient matrix. A method using electric charge as an excitation for the computation of the capacitance matrix is also proposed for reducing the computation time. The developed algorithm has been applied to simulate systems with power sources having high frequency and/or high d*v*/d*t*.**

***Keywords*—circuit, displacement current, electromagnetic field, finite element method, motor, parasitic capacitance, power electronic, transient.**

## I. Introduction

Nowadays the static power electronic driven electric motors (PE Drives) are replacing traditional motors excited by sinusoidal voltage in many applications. While these PE Drives provide new viability and new development opportunities of electric machines, they also bring new problems to users and researchers. As fast switching and repetitive steep rising or falling voltages of PE Drives have high-frequency contents, their parasitic capacitive effect and skin effect are very significant [1-4]. This factor leads to non-uniform voltage distribution among coils. The associated high d*v*/d*t* and high d*i*/d*t* stresses are sources of premature winding insulation failures. If the motor is connected to the inverter through possible long feeder cables, voltage doubling at the motor terminals, known as reflected wave phenomenon, will also seriously affect the performance of these motors [5-7].

Conventional models of electric machines operating under sinusoidal voltage excitations at power frequency cannot precisely consider high-frequency effects if the machines are energized by square wave voltage excitations. As the switching frequency increases, the influence of eddy-current in magnetic cores and the skin effects on windings will become increasingly significant in the modeling of electric machines and drives. Therefore, the modeling of PE Drives with all the above factors taken into account is highly desirable for the purpose of accurate numerical simulation.

In [8] and [9], electric circuit models are used to simulate the traveling waves and voltage distribution in electric motors. The disadvantage of these modeling is that the eddy-current effect and nonlinear iron cores cannot be included. To consider the magnetic field distributions, in [10] and [11], finite difference methods are developed; in [12], an eddy-current solver using FEM is proposed to simulate the magnetic field in the frequency domain.

The most suitable method to study such transient problems is to use the time stepping FEM coupling with electric circuit to compute the magnetic fields and the circuit system simultaneously. However such method is mainly limited to modeling low-frequency problems because the electric field is not coupled and the displacement current is ignored. To overcome this limitation, reference [13] presents a method which uses capacitances to include the effect of the displacement current. Reference [14] uses a similar method with the commercial software Maxwell 2D. Their methods cannot include the displacement current in the direction of the model's depth.

In this paper a 2-D FEM is proposed to include the parasitic capacitive effect, eddy-current effect and arbitrarily connected external circuits. The proposed new FEM formulation includes the displacement current in the direction of the model's depth, and represents the displacement current effect in the 2-D plane of the solution domain by connecting capacitances among conductors. For the computation of the capacitance matrix, a method using electric charge as an excitation is presented to reduce the computing time. It has been used to simulate the transient problems in which the electric sources have high frequency components.

## II. In the Region of Solid Conductors

The following hypotheses are introduced:

(1) The magnetic flux density $\vec{B}$ has components confined to the *x*-*y* plane. Therefore the magnetic vector potential $\vec{A}$ has a component in the *z* direction only, that is, $\vec{A} = A_z\vec{z}$; it is constant along the *z* axis. The coulomb gauge $\nabla \cdot \vec{A} = \frac{\partial A_z}{\partial z} = 0$ is satisfied.

(3) The conduction current flows along the *z* axis.

(4) The charge density is null.

### A. The Electric Field

The electric field can be decomposed into two orthogonal vectors:

$$\vec{E} = \vec{E}_z + \vec{E}_{xy} \tag{1}$$

For the component $E_z$ in the *z* direction:

$$E_z = -\frac{\partial A}{\partial t} - \frac{\partial V}{\partial z} \tag{2}$$

where $V$ is the electric scalar potential of the conductor in the domain of magnetic field. Equation (2) means that the changing magnetic field and the electric scalar potential produce electric field in the *z* direction. If $u_c$ is the voltage

**978-1-4244-1699-8/08/$25.00 ©2008 IEEE**

drop between the two terminals of the conductor with the length $l$ in the $z$ direction, one has:

$$\frac{\partial V}{\partial z} = -\frac{d_w}{l} u_c \tag{3}$$

where $d_w$ is the polarity (+1 or –1) to represent either the forward or return path. Substituting (3) into (2), one has:

$$E_z = -\frac{\partial A}{\partial t} + \frac{d_w}{l} u_c \tag{4}$$

Since the components $A_x$ and $A_y$ are neglected, one has:

$$\vec{E}_{xy} = -(\nabla V)_{xy} \tag{5}$$

It means that the magnetic field has no direct effect on the electric field on the *x-y* plane.

According to $\nabla \cdot \vec{D} = \rho$ and $\vec{D} = \varepsilon \vec{E}$, one has:

$$\nabla \cdot \vec{D}_{xy} = \nabla \cdot \varepsilon \vec{E}_{xy} = -\nabla \cdot (\varepsilon \nabla V)_{xy} = \rho \tag{6}$$

On the outside of the conductors, the charge density $\rho = 0$. In conductors, the electric relaxation time $\tau = \varepsilon/\sigma$ (= $8.854\times10^{-12}$ F/m / $5.8\times10^{7}$ siemens/meter in copper) is very small, hence it is assumed that $\rho = 0$. Each conductor is thus an equal-potential region in the *x-y* plane [15]. The electric field equation on the *x-y* plane is:

$$-\nabla_{xy} \cdot (\varepsilon \nabla_{xy} V) = 0 \tag{7}$$

*B. The Magnetic Field*

The electric vector displacement $E_z$ generates $J_{dz}$; then $J_{dz}$ generates $A_z$, which means the changing electric field generates a magnetic field in the *x-y* plane; $E_{xy}$ generates $J_{dxy}$, and $J_{dxy}$ generates $A_{xy}$. In the 2-D FEM the influence of $A_{xy}$ is negligible.

According to the Maxwell-Ampere's law:

$$\nabla \times (\nu \nabla \times \vec{A}) = \sigma \vec{E} + \varepsilon \frac{\partial \vec{E}}{\partial t} \tag{8}$$

and

$$\nabla \times (\nu \nabla \times \vec{A}) = -\nabla_{xy} \cdot (\nu \nabla_{xy} A_z) \tag{9}$$

one has:

$$-\nabla_{xy} \cdot (\nu \nabla_{xy} A) + \sigma \frac{\partial A}{\partial t} + \sigma \frac{\partial V}{\partial z} - \varepsilon \frac{\partial}{\partial t}\left(-\frac{\partial A}{\partial t} - \frac{\partial V}{\partial z}\right) = 0 \tag{10}$$

where $A_z$ is simplified as $A$; $\nu$ is the reluctivity of the material and $\sigma$ is the conductivity.

Therefore, substituting (3) into (10), the local magnetic field equation in the conductor can be written as:

$$-\nabla_{xy} \cdot (\nu \nabla_{xy} A) + \sigma \frac{\partial A}{\partial t} - \frac{d_w \sigma}{l} u_c + \varepsilon \frac{\partial^2 A}{\partial t^2} - \frac{d_w \varepsilon}{l} \frac{\partial u_c}{\partial t} = 0 \tag{11}$$

*C. The Current Branch Equation*

The total current density in the conductor along the direction of the $z$ axis is:

$$J_z = -d_w \sigma \frac{\partial A}{\partial t} - \sigma \frac{u_c}{l} + \varepsilon \frac{\partial}{\partial t}\left(-d_w \frac{\partial A}{\partial t} + \frac{u_c}{l}\right) \tag{12}$$

The total current in the conductor along the $z$ axis is:

$$i_c = \iint_{\Omega_c} \left[\sigma\left(-d_w \frac{\partial A}{\partial t} + \frac{u_c}{l}\right) + \varepsilon\left(-d_w \frac{\partial^2 A}{\partial t^2} + \frac{\partial}{\partial t}\frac{u_c}{l}\right)\right] \mathrm{d}\Omega$$

$$= -d_w \sigma \iint_{\Omega_c} \frac{\partial A}{\partial t} \mathrm{d}\Omega + \sigma \frac{\iint_{\Omega_c} \mathrm{d}\Omega}{l} u_c + \iint_{\Omega_c} \varepsilon\left(-d_w \frac{\partial^2 A}{\partial t^2} + \frac{\partial}{\partial t}\frac{u_c}{l}\right) \mathrm{d}\Omega$$

$$= e_c + \frac{1}{R_c} u_c + \iint_{\Omega_c} \varepsilon\left(-d_w \frac{\partial^2 A}{\partial t^2} + \frac{\partial}{\partial t}\frac{u_c}{l}\right) \mathrm{d}\Omega \tag{13}$$

where the resistance of the conductor:

$$R_c = \frac{l}{\sigma \iint_{\Omega_c} \mathrm{d}\Omega} = \frac{l}{\sigma S_c} \tag{14}$$

where $S_c = \iint_{\Omega_c} \mathrm{d}\Omega$ is the cross-sectional area of the conductor.

The back e.m.f. of the conductor is:

$$e_c = -d_w \sigma \iint_{\Omega_c} \frac{\partial A}{\partial t} \mathrm{d}\Omega \tag{15}$$

*D. The Current in the x-y Plane*

The current density in the *x-y* plane is:

$$\vec{J}_{xy} = \sigma \vec{E}_{xy} \tag{16}$$

The current flows out from the conductor in the *x-y* plane:

$$i_{xy} = \iint_S \frac{\partial}{\partial t} \vec{D} \cdot \mathrm{d}\vec{S} = \iint_S \frac{\partial}{\partial t} \vec{D} \cdot \vec{n} \mathrm{d}S = \left(\frac{\mathrm{d}Q}{\mathrm{d}t}\right) \tag{17}$$

where $S$ is the cylindrical external surface of the conductor and $Q$ is the charge. In 2-D, equation (17) is simplified as:

$$i_{xy} = l \oint_\Gamma \varepsilon \frac{\partial}{\partial t} \vec{E}_{xy} \cdot \vec{n} \mathrm{d}l \tag{18}$$

This line integration is along $\Gamma$, which is the contour of the conductor in the *x-y* plane.

The $i_{xy}$ is the current flowing out from the conductor via capacitive effect. For simplicity, the electrostatic field described by (7) is first solved; then the capacitance matrix is extracted. The current flowing out from the conductor $n$ in the $x$-$y$ plane can be computed by:

$$i_{xyn} = \sum_{k=1}^{\text{All conductors}} C_{nk} \frac{\mathrm{d}u_{nk}}{\mathrm{d}t} \tag{19}$$

The electrostatic field with multi right hand sides (see Section VII) only needs to be computed once if there is no motion. Under such condition, only the electric circuit with all these capacitances, instead of the electric field, needs to be coupled with the magnetic field directly.

*E. The Equations of One Conductor*

To overcome the problem that equation (11) includes the second derivative of $A$ with respect to time $t$, and to keep the coefficient matrix of the last system equations symmetrical, the unknown $E_z$ is kept in the system equation. Multiplying $\varepsilon$ to the two sides of (4), one has:

$$-\varepsilon \frac{\partial A}{\partial t} - \varepsilon E_z + \frac{d_w \varepsilon}{l} u_c = 0 \tag{20}$$

According to (4) and (11), one has:

$$-\nabla_{xy} \cdot (\nu \nabla_{xy} A) + \sigma \frac{\partial A}{\partial t} - \varepsilon \frac{\partial E_z}{\partial t} - \frac{d_w \sigma}{l} u_c = 0 \tag{21}$$

According to (13), one has:

$$-\frac{d_w \sigma}{l} \iint_{\Omega_c} \frac{\partial A}{\partial t} \mathrm{d}\Omega + \frac{1}{l R_c} u_c + \frac{d_w \varepsilon}{l} \iint_{\Omega_c} \frac{\partial E_z}{\partial t} \mathrm{d}\Omega = \frac{1}{l} i_c \tag{22}$$

The system equations in the region of solid conductors are (21), (20) and (22).

*F. The Grouped Conductors*

Periodic boundary conditions can be used to reduce the solution domain. Similar to the stranded windings, the solid conductors should also be grouped together if their electric

and magnetic field quantities satisfy either periodic condition or anti-periodic condition [16]. The basic relationships between one conductor and the conductor group are:

$$S_c = \frac{pS_w}{N_w} \tag{23}$$

$$i_c = \frac{i_w}{a} \tag{24}$$

$$u_c = \frac{a}{N_w} u_w \tag{25}$$

$$R_c = \frac{a^2}{N_w} R_w \tag{26}$$

where $p$ is the symmetry multiplier which is defined as the ratio of the original full cross-sectional area to the solution area; $S_w = \iint_{\Omega_w} \mathrm{d}\Omega$ is the total cross-sectional area of the region occupied by this conductor group in the solution domain; $u_w$ is the voltage difference between the two terminals of the solid conductor group; $i_w$ is the total current; $N_w$ is the total conductor number; $a$ is the number of parallel branches and $R_w$ is the d.c. resistance of the conductor group.

Substituting (25) into (21), the field equation in the solid conductor group is:

$$-\nabla_{xy} \cdot \left(\nu \nabla_{xy} A\right) + \sigma \frac{\partial A}{\partial t} - \varepsilon \frac{\partial E_z}{\partial t} - \frac{d_w a \sigma}{N_w l} u_w = 0 \tag{27}$$

Substituting (25) into (20), one has:

$$-\varepsilon \frac{\partial A}{\partial t} - \varepsilon E_z + \frac{a\varepsilon}{N_w l} u_w = 0 \tag{28}$$

Substituting (23), (24), (25) and (26) into (22), the circuit branch equation of the solid conductor group is:

$$-\frac{d_w a \sigma}{N_w l} \iint_{\Omega_w} \frac{\partial A}{\partial t} \mathrm{d}\Omega + \frac{1}{lpR_w} u_w + \frac{a\varepsilon}{N_w l} \iint_{\Omega_w} \frac{\partial E_z}{\partial t} \mathrm{d}\Omega = \frac{1}{lp} i_w \tag{29}$$

Therefore, the system equations in the region of the solid conductors are (27), (28) and (29).

## III. In the Region of Stranded Windings

### A. The Magnetic Field Equation

All conductors in the same stranded winding are grouped together. The magnetic field equation in the region of the stranded windings can be expressed as:

$$\nabla_{xy} \cdot \left(\nu \nabla_{xy} A\right) + \frac{d_w N_w}{S_w a p} i_w = 0 \tag{30}$$

where $i_w$ is the winding current; $S_w$ is the total cross-sectional area of the region occupied by this coil group in the solution domain; $N_w$ is the total conductor number of this winding and $a$ is the number of parallel branches in this winding.

### B. The Circuit Branch Equation

The branch equation of the stranded windings is:

$$\frac{d_w N_w l}{S_w a} \iint_{\Omega} \frac{\partial A}{\partial t} \mathrm{d}\Omega + R_w i_w = u_w \tag{31}$$

where $u_w$ is the voltage on the two terminals of the winding; $l$ is the model depth in the $z$ axis; and $R_w$ is the total d.c. resistance of the winding:

$$R_w = \frac{N_w^2}{a^2 p} \frac{l}{\sigma S_w} \tag{32}$$

In the region of the stranded windings, according to the branch equation (31) of the stranded windings, one has:

$$i_w = \frac{-e + u_w}{R_w} \tag{33}$$

where $e$ is the back e.m.f.:

$$e = \frac{d_w N_w l}{S_w a} \iint_{\Omega} \frac{\partial A}{\partial t} \mathrm{d}\Omega \tag{34}$$

Substituting (33) into (30), the field equation becomes:

$$\nabla_{xy} \cdot \left(\nu \nabla_{xy} A\right) - \frac{d_w a \sigma}{N_w l} e + \frac{d_w a \sigma}{N_w l} u_w = 0 \tag{35}$$

Equation (34) can also be written as

$$\frac{d_w a \sigma}{N_w l} \iint_{\Omega} \frac{\partial A}{\partial t} \mathrm{d}\Omega - \frac{1}{lpR_w} e = 0 \tag{36}$$

The branch equation (31) can be written as:

$$\frac{d_w a \sigma}{N_w l} \iint_{\Omega} \frac{\partial A}{\partial t} \mathrm{d}\Omega - \frac{1}{lpR_w} u_w = -\frac{1}{lp} i_w \tag{37}$$

Equations (35), (36) and (37) are the basic equations for the stranded windings. The additional unknown $e$ is introduced to keep the coefficient matrix of the system equations symmetrical.

## IV. In the Other Regions

In regions of air and iron, and also in regions having permanent magnets (PM) and electric current densities, the field diffusion equation is:

$$\nabla_{xy} \cdot \left(\nu \nabla_{xy} A\right) - \sigma \frac{\partial A}{\partial t} = -J_s + \nu \mu_0 \left( \frac{\partial M_x}{\partial y} - \frac{\partial M_y}{\partial x} \right) \tag{38}$$

where the first term in the right hand side only exists in regions having electric current densities; the second term in the right hand side only exists in PM; $\nu$ equals to the equivalent reluctivity in the PM; $\mu_0$ is the magnetic permeability in vacuum; $M_x$ and $M_y$ are, respectively, the $x$ and $y$ components of the magnetization vector (amperes/meter) in the PM.

## V. The Matrix Form of Field Equations

### A. Summary of Field Equations

The basic equations in all regions can be summarized as:

$$-\nabla_{xy} \cdot \left(\nu \nabla_{xy} A\right) + \sigma \frac{\partial A}{\partial t} - \varepsilon \frac{\partial E_z}{\partial t} + \frac{d_w a \sigma}{N_w l} e - \frac{d_w a \sigma}{N_w l} u_w = J_s - \nu \mu_0 \left( \frac{\partial M_x}{\partial y} - \frac{\partial M_y}{\partial x} \right) \quad \text{(magnetic field equation)} \tag{39}$$

$$-\varepsilon \frac{\partial A}{\partial t} - \varepsilon E_z + \frac{a\varepsilon}{N_w l} u_w = 0 \quad \text{(electric field equation)} \tag{40}$$

$$\frac{d_w a \sigma}{N_w l} \iint_{\Omega_w} \frac{\partial A}{\partial t} \mathrm{d}\Omega - \frac{1}{lpR_w} e = 0 \quad \text{(additional equation)} \tag{41}$$

$$-\frac{d_w a \sigma}{N_w l} \iint_{\Omega_w} \frac{\partial A}{\partial t} \mathrm{d}\Omega + \frac{a\varepsilon}{N_w l} \iint_{\Omega_w} \frac{\partial E_z}{\partial t} \mathrm{d}\Omega + \frac{1}{lpR_w} u_w = \frac{1}{lp} i_w \quad \text{(branch equation)} \tag{42}$$

where $i_w$ is the current in the stranded windings or the solid conductor groups and $u_w$ is the voltage difference between the two terminals of the stranded windings or the solid conductor groups. The fourth term on the left side of the field equation (39), and also the additional equation (41) only exist in the stranded winding region. The second and the third terms in the

left side of (39), the electric field equation (40), and the second term in the branch equation (42) only exist in the solid conductor region.

*B. The Matrix Form of Field Equations*

After applying a standard Galerkin procedure, the coupled field and circuit branch equations in the magnetic field region can be written in block matrix format:

$$\begin{bmatrix} \boldsymbol{C}_{11} & 0 & \boldsymbol{C}_{13} & \boldsymbol{C}_{14} \\ 0 & \boldsymbol{C}_{22} & 0 & \boldsymbol{C}_{24} \\ 0 & 0 & \boldsymbol{C}_{33} & 0 \\ 0 & 0 & 0 & \boldsymbol{C}_{44} \end{bmatrix} \begin{Bmatrix} A \\ E_z \\ e \\ u_w \end{Bmatrix} + \begin{bmatrix} \boldsymbol{D}_{11} & \boldsymbol{D}_{12} & 0 & 0 \\ \boldsymbol{D}_{21} & 0 & 0 & 0 \\ \boldsymbol{D}_{31} & 0 & 0 & 0 \\ \boldsymbol{D}_{41} & \boldsymbol{D}_{42} & 0 & 0 \end{bmatrix} \begin{Bmatrix} \frac{\mathrm{d}\boldsymbol{A}}{\mathrm{d}t} \\ \frac{\mathrm{d}\boldsymbol{E}_z}{\mathrm{d}t} \\ \frac{\mathrm{d}\boldsymbol{e}}{\mathrm{d}t} \\ \frac{\mathrm{d}\boldsymbol{u}_w}{\mathrm{d}t} \end{Bmatrix} = \begin{Bmatrix} 0 \\ 0 \\ 0 \\ \frac{1}{lp}\boldsymbol{i}_w \end{Bmatrix} + \begin{Bmatrix} \boldsymbol{P}_1 \\ 0 \\ 0 \\ 0 \end{Bmatrix} \tag{43}$$

The coefficients associated with the degree of freedoms (DoFs) of $A_i$, $A_j$ and $i_{w(n)}$ (here the subscript $i$, $j$ and $n$ are the indexes of the unknowns) are:

$$C_{11ij} = \iint_{\Omega_e} \nu \left( \frac{\partial N_i}{\partial x}\frac{\partial N_j}{\partial x} + \frac{\partial N_i}{\partial y}\frac{\partial N_j}{\partial y} \right) \mathrm{d}x\mathrm{d}y \tag{44}$$

$$D_{11ij} = \iint_{\Omega_e} \sigma N_i N_j \mathrm{d}x\mathrm{d}y \tag{45}$$

$$D_{12in} = D_{21ni} = -\varepsilon \iint_{\Omega_e} N_i \mathrm{d}x\mathrm{d}y \tag{46}$$

$$C_{24\,in} = \frac{a\varepsilon}{N_w l} \iint_{\Omega_e} N_i \mathrm{d}x\mathrm{d}y \tag{47}$$

$$C_{13\,in} = -C_{14\,in} = \frac{d_w a \sigma}{N_w l} \iint_{\Omega_e} N_i \mathrm{d}x\mathrm{d}y \tag{48}$$

$$C_{22ii} = -\varepsilon \iint_{\Omega_e} N_i \mathrm{d}x\mathrm{d}y \tag{49}$$

$$C_{33n} = -C_{44n} = -\frac{1}{lpR_{w(n)}} \tag{50}$$

$$D_{31ni} = -D_{41ni} = \frac{d_w a \sigma}{N_w l} \iint_{\Omega_e} N_i \mathrm{d}x\mathrm{d}y \tag{51}$$

$$P_{1i} = \int_{C_e} N_i H_t \mathrm{d}c + \iint_{\Omega_e} N_i \left[ J_s - \nu\mu_0 \left( \frac{\partial M_x}{\partial y} - \frac{\partial M_y}{\partial x} \right) \right] \mathrm{d}x\mathrm{d}y \tag{52}$$

where $N_i$ is the shape function. $H_t = \nu \dfrac{\partial A}{\partial n}$ and the first term on the right hand side of (52) only exist on non-zero Neumann boundary conditions. It is observed that $\boldsymbol{C}_{11} = \boldsymbol{C}_{11}^T$, $\boldsymbol{C}_{22} = \boldsymbol{C}_{22}^T$, $\boldsymbol{C}_{33} = \boldsymbol{C}_{33}^T$, $\boldsymbol{C}_{44} = \boldsymbol{C}_{44}^T$, $\boldsymbol{D}_{11} = \boldsymbol{D}_{11}^T$, $\boldsymbol{D}_{12} = \boldsymbol{D}_{21}^T$, $\boldsymbol{C}_{24} = \boldsymbol{D}_{42}^T$, $\boldsymbol{C}_{13} = \boldsymbol{D}_{31}^T$ and $\boldsymbol{C}_{14} = \boldsymbol{D}_{41}^T$.

## VI. Coupling with External Circuit

Both the circuit equations of the windings in the field region and the external circuit will be coupled with the magnetic field equations together and solved simultaneously.

*A. The External Circuit Equation*

In time domain all inductance and capacitance are expressed as equivalent resistance. The branch equation of the external circuit at each time step can be simplified as:

$$[G_e]\{u_e\} = \{i_e\} + \{P_e\} \tag{53}$$

where $u_e$ and $i_e$ are the branch voltage and current, respectively; $G_e$ is the matrix of the conductance; $P_e$ is the column matrix associated with voltage sources, current sources as well as the solution from the previous time step for inductive and capacitive elements.

*B. The Coupled System Equations*

Using the backward Euler's method to discretize the time variable and multiplying the time step size $\Delta t$ to the additional equation and the branch equation, one obtains the recurrence formulas of the $k^{\text{th}}$ step for the time stepping process as follows:

$$\begin{bmatrix} \boldsymbol{C}_{11} + \frac{\boldsymbol{D}_{11}}{\Delta t} & \frac{\boldsymbol{D}_{12}}{\Delta t} & \boldsymbol{C}_{13} & \boldsymbol{C}_{14} \\ \frac{\boldsymbol{D}_{12}^T}{\Delta t} & \boldsymbol{C}_{22} & 0 & \boldsymbol{C}_{24} \\ \boldsymbol{C}_{13}^T & 0 & \Delta t\boldsymbol{C}_{33} & 0 \\ \boldsymbol{C}_{14}^T & \boldsymbol{C}_{24}^T & 0 & \Delta t\boldsymbol{C}_{44} \end{bmatrix} \begin{Bmatrix} \boldsymbol{A}^k \\ \boldsymbol{E}_z^k \\ \boldsymbol{e}^k \\ \boldsymbol{u}_w^k \end{Bmatrix} = \begin{Bmatrix} 0 \\ 0 \\ 0 \\ \frac{\Delta t}{lp}\boldsymbol{i}_w^k \end{Bmatrix} + \begin{Bmatrix} \boldsymbol{P}_1 + \frac{\boldsymbol{D}_{11}}{\Delta t}\boldsymbol{A}^{k-1} + \frac{\boldsymbol{D}_{12}}{\Delta t}\boldsymbol{E}_z^{k-1} \\ \frac{\boldsymbol{D}_{12}^T}{\Delta t}\boldsymbol{E}_z^{k-1} \\ \boldsymbol{C}_{13}^T\boldsymbol{A}^{k-1} \\ \boldsymbol{C}_{14}^T\boldsymbol{A}^{k-1} + \boldsymbol{C}_{24}^T\boldsymbol{E}_z^{k-1} \end{Bmatrix} \tag{54}$$

where the superscript $k$ indicates the appropriate values at the $k^{\text{th}}$ step of the time stepping computation.

Multiplying $\Delta t/lp$ to the two sides of (53), one has the branch equation of the external circuit:

$$\left[\frac{\Delta t}{lp}\boldsymbol{G}_e\right]\{\boldsymbol{u}_e\} = \left\{\frac{\Delta t}{lp}\boldsymbol{i}_e\right\} + \left\{\frac{\Delta t}{lp}\boldsymbol{P}_e\right\} \tag{55}$$

Adding the external circuit equation (55) into (54), one obtains:

$$\begin{bmatrix} \boldsymbol{C}_{11} + \frac{\boldsymbol{D}_{11}}{\Delta t} & \frac{\boldsymbol{D}_{12}}{\Delta t} & \boldsymbol{C}_{13} & \boldsymbol{C}_{14} & 0 \\ \frac{\boldsymbol{D}_{12}^T}{\Delta t} & \boldsymbol{C}_{22} & 0 & \boldsymbol{C}_{24} & 0 \\ \boldsymbol{C}_{13}^T & 0 & \Delta t\boldsymbol{C}_{33} & 0 & 0 \\ \boldsymbol{C}_{14}^T & \boldsymbol{C}_{24}^T & 0 & \Delta t\boldsymbol{C}_{44} & 0 \\ 0 & 0 & 0 & 0 & \frac{\Delta t}{lp}\boldsymbol{G}_e \end{bmatrix} \begin{Bmatrix} \boldsymbol{A}^k \\ \boldsymbol{E}_z^k \\ \boldsymbol{e}^k \\ \boldsymbol{u}_w^k \\ \boldsymbol{u}_e^k \end{Bmatrix} = \begin{Bmatrix} 0 \\ 0 \\ 0 \\ \frac{\Delta t}{lp}\boldsymbol{i}_w^k \\ \frac{\Delta t}{lp}\boldsymbol{i}_e^k \end{Bmatrix} + \begin{Bmatrix} \boldsymbol{P}_1 + \frac{\boldsymbol{D}_{11}}{\Delta t}\boldsymbol{A}^{k-1} + \frac{\boldsymbol{D}_{12}}{\Delta t}\boldsymbol{E}_z^{k-1} \\ \frac{\boldsymbol{D}_{12}^T}{\Delta t}\boldsymbol{E}_z^{k-1} \\ \boldsymbol{C}_{13}^T\boldsymbol{A}^{k-1} \\ \boldsymbol{C}_{14}^T\boldsymbol{A}^{k-1} + \boldsymbol{C}_{24}^T\boldsymbol{E}_z^{k-1} \\ \frac{\Delta t}{lp}\boldsymbol{P}_e \end{Bmatrix} \tag{56}$$

The branch voltage column matrix and the branch current column matrix are:

$$\{\boldsymbol{u}_b\} = \begin{Bmatrix} \boldsymbol{u}_w \\ \boldsymbol{u}_e \end{Bmatrix} \tag{57}$$

$$\{\boldsymbol{i}_b\} = \begin{Bmatrix} \boldsymbol{i}_w \\ \boldsymbol{i}_e \end{Bmatrix} \tag{58}$$

Using the nodal method, the relationship between the

branch voltage $u_b$ and the nodal voltage $u_n$ is:

$$\{\boldsymbol{u}_b\} = [\boldsymbol{A}_{nb}^T]\{\boldsymbol{u}_n\} \tag{59}$$

where $\boldsymbol{A}_{nb}$ is the node-to-branch incidence matrix.

The Kirchhoff's current law can be expressed as,

$$[\boldsymbol{A}_{nb}]\{\boldsymbol{i}_b\} = 0 \tag{60}$$

The matrix $\boldsymbol{A}_{nb}$ can be written as:

$$[\boldsymbol{A}_{nb}] = [\boldsymbol{A}_{nw} \quad \boldsymbol{A}_{ne}] \tag{61}$$

where $\boldsymbol{A}_{nw}$ is the node-to-branch incidence matrix of the windings and $\boldsymbol{A}_{ne}$ is the node-to-branch incidence matrix of the external circuit.

The equation (59) can be written as:

$$\begin{Bmatrix} \boldsymbol{u}_w \\ \boldsymbol{u}_e \end{Bmatrix} = \begin{bmatrix} \boldsymbol{A}_{nw}^T \\ \boldsymbol{A}_{ne}^T \end{bmatrix} \{\boldsymbol{u}_n\} \tag{62}$$

The Kirchhoff's current law can be expressed as,

$$[\boldsymbol{A}_{nw} \quad \boldsymbol{A}_{ne}] \begin{Bmatrix} \boldsymbol{i}_w \\ \boldsymbol{i}_e \end{Bmatrix} = 0 \tag{63}$$

Substituting the relationships (62) and (63) into the system equations (56), the final global equations are obtained:

$$\begin{bmatrix} \boldsymbol{C}_{11} + \dfrac{\boldsymbol{D}_{11}}{\Delta t} & \dfrac{\boldsymbol{D}_{12}}{\Delta t} & \boldsymbol{C}_{13} & \boldsymbol{C}_{14}\boldsymbol{A}_{nw}^T \\ \dfrac{\boldsymbol{D}_{12}^T}{\Delta t} & \boldsymbol{C}_{22} & 0 & \boldsymbol{C}_{24}\boldsymbol{A}_{ne}^T \\ \boldsymbol{C}_{13}^T & 0 & \Delta t\boldsymbol{C}_{33} & 0 \\ \boldsymbol{A}_{nw}\boldsymbol{C}_{14}^T & \boldsymbol{A}_{nw}\boldsymbol{C}_{24}^T & 0 & \boldsymbol{A}_{nw}\Delta t\boldsymbol{C}_{44}\boldsymbol{A}_{nw}^T + \boldsymbol{A}_{ne}\dfrac{\Delta t}{lp}\boldsymbol{G}_e\boldsymbol{A}_{ne}^T \end{bmatrix} \begin{Bmatrix} \boldsymbol{A}^k \\ \boldsymbol{E}_z^k \\ \boldsymbol{e}^k \\ \boldsymbol{u}_n^k \end{Bmatrix}$$

$$= \begin{Bmatrix} \boldsymbol{P}_1 + \dfrac{\boldsymbol{D}_{11}}{\Delta t}\boldsymbol{A}^{k-1} + \dfrac{\boldsymbol{D}_{12}}{\Delta t}\boldsymbol{E}_z^{k-1} \\ \dfrac{\boldsymbol{D}_{12}^T}{\Delta t}\boldsymbol{E}_z^{k-1} \\ \boldsymbol{C}_{13}^T\boldsymbol{A}^{k-1} \\ \boldsymbol{A}_{nw}\left(\boldsymbol{C}_{14}^T\boldsymbol{A}^{k-1} + \boldsymbol{C}_{24}^T\boldsymbol{E}_z^{k-1}\right) + \boldsymbol{A}_{ne}\left(\dfrac{\Delta t}{lp}\boldsymbol{P}_e\right) \end{Bmatrix} \tag{64}$$

where the coefficient matrix is symmetrical.

## VII. Capacitance Matrix Computation

The electric filed equation on the *x*-*y* plane is:

$$\nabla_{xy} \cdot \left(\varepsilon \nabla_{xy} V\right) = -\rho \tag{65}$$

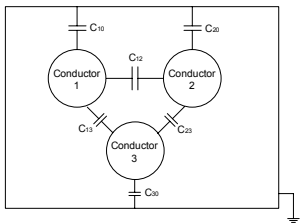


Fig. 1. The capacitances among three conductors

For simplicity, a system with three conductors as shown in Fig. 1 is taken as an example. Usually the capacitances are computed by solving the field equations 3 times when setting the voltage potentials as: ($V_1$, $V_2$, $V_3$) = (1, 0, 0), (0, 1, 0) and (0, 0, 1), respectively (here $V_1$, $V_2$, $V_3$ are the voltage potentials on the conductor 1, 2 and 3, respectively). Because such setting of the voltage potentials is taken as constraints in (65), it is not convenient in FEM programming.

Here the charge excitation is used to calculate the capacitances. Because of the relationship of $Q = CV$, the net charge on each object is:

$$\begin{Bmatrix} Q_1 \\ Q_2 \\ Q_3 \end{Bmatrix} = \begin{bmatrix} C_{10} + C_{12} + C_{13} & -C_{12} & -C_{13} \\ -C_{21} & C_{20} + C_{21} + C_{23} & -C_{23} \\ -C_{31} & -C_{32} & C_{30} + C_{31} + C_{32} \end{bmatrix} \begin{Bmatrix} V_1 \\ V_2 \\ V_3 \end{Bmatrix}$$

$$= \begin{bmatrix} C_{11} & -C_{12} & -C_{13} \\ -C_{21} & C_{22} & -C_{23} \\ -C_{31} & -C_{32} & C_{33} \end{bmatrix} \begin{Bmatrix} V_1 \\ V_2 \\ V_3 \end{Bmatrix} \tag{66}$$

By defining a *G* matrix:

$$\begin{bmatrix} G_{11} & G_{12} & G_{13} \\ G_{21} & G_{22} & G_{23} \\ G_{31} & G_{32} & G_{33} \end{bmatrix} = \begin{bmatrix} C_{11} & -C_{12} & -C_{13} \\ -C_{21} & C_{22} & -C_{23} \\ -C_{31} & -C_{32} & C_{33} \end{bmatrix}^{-1} \tag{67}$$

one has:

$$\begin{Bmatrix} V_1 \\ V_2 \\ V_3 \end{Bmatrix} = \begin{bmatrix} C_{11} & -C_{12} & -C_{13} \\ -C_{21} & C_{22} & -C_{23} \\ -C_{31} & -C_{32} & C_{33} \end{bmatrix}^{-1} \begin{Bmatrix} Q_1 \\ Q_2 \\ Q_3 \end{Bmatrix} = \begin{bmatrix} G_{11} & G_{12} & G_{13} \\ G_{21} & G_{22} & G_{23} \\ G_{31} & G_{32} & G_{33} \end{bmatrix} \begin{Bmatrix} Q_1 \\ Q_2 \\ Q_3 \end{Bmatrix} \tag{68}$$

If the charge excitations are set as:

$$\{Q_1 \quad Q_2 \quad Q_3\}^T = \{1 \quad 0 \quad 0\}^T \tag{69}$$

one has:

$$\begin{bmatrix} V_1 \\ V_2 \\ V_3 \end{bmatrix} = \begin{bmatrix} G_{11} & G_{12} & G_{13} \\ G_{21} & G_{22} & G_{23} \\ G_{31} & G_{32} & G_{33} \end{bmatrix} \begin{bmatrix} 1 \\ 0 \\ 0 \end{bmatrix} \tag{70}$$

After the field is solved, $V_1$, $V_2$ and $V_3$ are known. Then one has:

$$\{G_{11} \quad G_{21} \quad G_{31}\}^T = \{V_1 \quad V_2 \quad V_3\}^T \tag{71}$$

Similarly, If the charge excitations are set as:

$$\{Q_1 \quad Q_2 \quad Q_3\}^T = \{0 \quad 1 \quad 0\}^T \tag{72}$$

one has:

$$\{G_{12} \quad G_{22} \quad G_{32}\}^T = \{V_1 \quad V_2 \quad V_3\}^T \tag{73}$$

If the charge excitations are set as:

$$\{Q_1 \quad Q_2 \quad Q_3\}^T = \{0 \quad 0 \quad 1\}^T \tag{74}$$

one has:

$$\{G_{13} \quad G_{23} \quad G_{33}\}^T = \{V_1 \quad V_2 \quad V_3\}^T \tag{75}$$

After the *G* matrix is obtained, the *C* matrix can be obtained by (67). Using this algorithm, the coefficient matrix of the FEM equations can be kept the same. Only a multi right hand side problem needs to be solved. Therefore, the computing time to extract the capacitance matrix can be reduced.

## VIII. An Example

The developed FEM is applied to simulate the response of a step voltage – feeder cable – coil system. Fig. 2 shows one side of a coil with 8 turns in a slot. All solid conductors are connected as shown in Fig. 3. The turn-to-ground capacitance and turn-to-turn capacitance are computed first using electrostatic field solver as a pre-processor. The capacitance between non-adjacent turns is negligible.

The effect of the long feeder cable between the source and the coil is included in the simulation to study the impedance mismatch between the cable and the motor. Here the cable is

modeled as a circuit with a series of cascaded lumped parameter sections as shown in Fig. 4. The cable circuit and the coil circuit are connected together by the external circuit coupling with electromagnetic field.

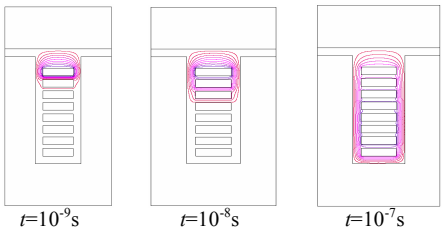


Fig. 2. Slot section of a form-wound coil and its flux plots

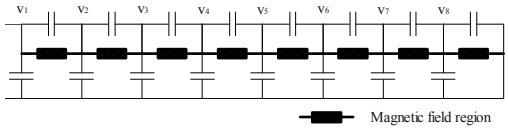


Fig. 3. Coil circuit

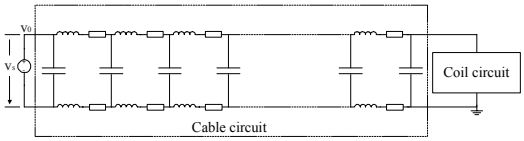


Fig. 4. The coil is connected to the step voltage through a long cable

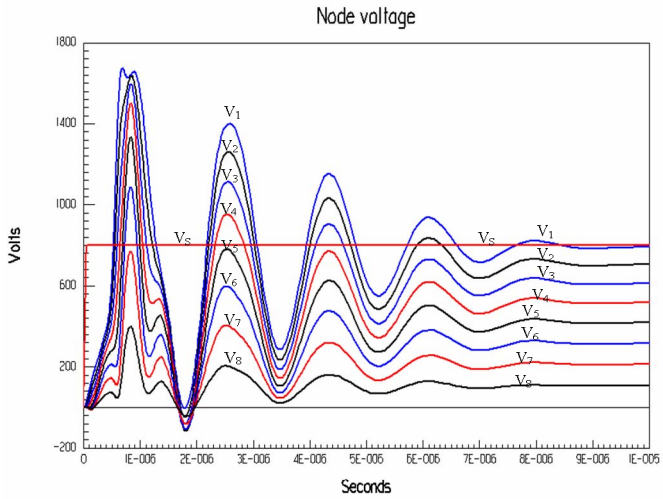


Fig. 5. Nodal voltage potential distribution

A step voltage (simulating the PWM wavefront; it is $V_s$ in Fig. 4 and Fig. 5) having 50 ns rise-time and 800 V magnitude is applied to the terminal of the coil. The simulated transient nodal voltage potentials are shown in Fig. 5 when the step voltage is applied to the coil terminal through a cable with a length of 100 m. The meanings of the voltage potentials $V_1$, $V_2$, …, $V_8$ in the Fig. 5 can be found in the Fig. 3. The voltage doubling phenomena at the coil terminal can be clearly observed from the waveforms.

## IX. Conclusions

A 2-D FEM for the electromagnetic field computation of power electronic drives is deduced, which can include the displacement current in the model's depth. The proposed model represents the displacement current effect on the plane of the solution domain by coupling the capacitance circuit with FEM equations. The capacitance matrix can be extracted by solving the electric field equations driven by charges, so only a set of equations with multi right hand sides needs to be solved for the capacitance matrix computation. The developed method is used to simulate the steep-fronted voltage applied to a coil connected by a feeder cable. It reveals that the voltage drops on the conductors are not uniform if the rise-time is very short. It also shows that the voltage on the terminal of the coil may be much higher than the voltage applied to the terminal of the feeder cable. The method can also be applied to study electromechanical equipments when they are subject to pulse sources or surge waves from thunderstorm or circuit breakers.

## References


[1] H. Bonnett, "Analysis of the impact of pulse-width modulated inverter voltage waveforms on ac induction motors," *IEEE Trans. Ind. Applicat.*, vol.32, pp.386-392, Mar./Apr. 1996.

[2] J. Melhorn, L. Tang, "Transient effects of PWM drives on induction motors," *IEEE/I&CPS Conf. Rec.*, pp.1-7, May 1995.

[3] R. J. Kerkman, D. Leggate, D. Schlegel, G. Skibinski, "PWM inverters and their influence on motor over-voltages," *IEEE APEC Conf. Rec.*, pp.103-113, 1997.

[4] M. Melfi, J. Sung, S. Bell, G. Skibinski, "Effect of surge voltage rise-time on the insulation of low voltage machines fed by PWM converters," *IEEE IAS Conf. Rec.*, pp.239-246, 1997.

[5] E. Persson, "Transient effects in application of PWM inverters to induction motors," *IEEE Trans. Ind. Applicat.*, vol.28, pp.1095-1101, Sept./Oct. 1992.

[6] R. Kerkman, D. Leggate, G. Skibinski, "Interaction of drive modulation and cable parameters on AC motor transients," *IEEE IAS Conf. Proc.*, pp.143-152, 1996.

[7] G. Skibinski, D. Leggate, R. J. Kerkman, "Cable characteristics and their influence on motor over-voltages," *IEEE APEC Conf. Rec.*, pp.114-121, 1997.

[8] L. Gubbala, A. von Jouanne, P. N. Enjeti, C. Singh, H. A. Toliyat, "Voltage distribution in the windings of an ac motor subjected to high dv/dt PWM voltages," *IEEE PESC Conf. Proc.*, pp.579-585, 1995.

[9] Hussain, G. Joos, "Modeling and simulation of traveling waves in induction motor drives," *IEEE APEC Conf. Rec.*, pp.128-134, 1997.

[10] D. B. Hyypio, "Simulation of cable and winding response to steep-fronted voltage waves," *IEEE IAS Conf. Rec.*, pp.800-806, 1995.

[11] Y. Tang, "Analysis of steep-fronted voltage distribution and turn insulation failure in inverter fed ac motor," *IEEE IAS Conf. Rec.*, pp.509-516, 1997.

[12] G. Suresh, H.A. Toliyat, D.A. Rendusara and P.N. Enjeti, "Predicting the transient effects of PWM voltage waveform on the stator windings of random wound induction motors," IEEE Trans. on Power Electronics, Vol.14, No.1, Jan. 1999, pp.23-30.

[13] J.F. Charpentier, Y. Lefevre and M. Lajoie-Mazenc, "A 2D Finite Element Formulation for the Study of the High Frequency Behaviour of Wound Components," *IEEE Trans. Magn.* Vol.32, No.3, May 1996, pp.1098-1101.

[14] H. A. Toliyat, G. Suresh, A. Abur, "Simulation of voltage stress on the inverter fed induction motor windings supplied through feeder cable," *IEEE IAS Conf. Rec.*, pp.143-150, 1997.

[15] R. Miller, D.M. Ryder and K.J. Overshott, "The Effect of High-Voltage Lightning Impulses on the Core Properties of Transformers," *IEEE Trans. Magn.* Vol.25, No.5, Sept. 1989, pp.3988-3990.

[16] W. N. Fu, P. Zhou, D. Lin, S. Stanton and Z. J. Cendes, "Modeling of Solid Conductors in Two-Dimensional Transient Finite-Element Analysis and Its Application to Electric Machines," *IEEE Trans. Magn.* Vol.40, No.2, March 2004, pp.426-434.